# RSC Advances

ROYAL SOCIETY
OF CHEMISTRY

www.rsc.org/advances

# Journal Name

## COMMUNICATION

# Versatile Heavy Metals Removal *via* Magnetic Mesoporous Nanocontainers†

S. Dib,[a] M. Boufatit,[a] S. Chelouaou,[a] F. Sadi-Hassaine,[a] J. Croissant,*[b] J. Long,[b] L. Raehm,[b] C. Charnay,[b] and J-O. Durand.[b]

**Versatile heavy metal ions removal is performed *via* iron oxide core mesoporous silica shell nanocontainers functionalized with diethylene triamine pentaacetic acid. Magnetic separation from aqueous media is obtained for a dozen of the most toxic heavy metal ions with remarkable efficiencies. Furthermore, this study demonstrates enhancement of the adsorption capacities with a combination of porous and surface functionalization of the nanocontainers.**

Heavy metal contamination from industrial processes and products has become a public health and environmental concern throughout the world.[1-6] Although there is no clear and scientific definition of heavy metals, it generally refers to metals having a specific density of more than 5 g.cm$^{-3}$.[1] In the year 2000, the European Union has legislated that "'heavy metal' means any compound of antimony, arsenic, cadmium, chromium(VI), copper, lead, mercury, nickel, selenium, tellurium, thallium and tin, as well as these materials in metallic form, as far as these are classified as dangerous substances."[7] The toxicity for human health of heavy metal ions, among which lead, cadmium, mercury and arsenic are considered to be the most dangerous,[1] can damage mental and central nervous functions. Besides, the essentiality of metal ions transport (e.g. copper, zinc, lead) *via* proteins for cellular biochemical processes in the body, can also become the Trojan horse for toxic metal ions accumulation. As a result, various damages can be caused by heavy metal ions to vital organs such as the lungs, the kidneys, and the liver.[8-11] Therefore, many devices have been elaborated to remove such ions, mainly ion-exchange materials,[12-14] membrane filtration and adsorption,[5, 15-17] and colloidal adsorbents.[18-22]

Superior efficiencies are obtained *via* adsorbents, [18, 23-25] and porous colloids would be most appropriate due to their high surface area, and the variability of surface modifications.[19] One challenge that colloidal adsorbents face is to separate the particles after ion adsorption. An efficient method utilizes the magnetic properties of iron oxide nanocrystals ($Fe_3O_4$NCs).[22, 26, 27] Note that, for such an application $Fe_3O_4$NCs must be coated in order to avoid iron ions leaching in the waste solutions. Besides, to enhance the pollutant removal capacities of $Fe_3O_4$NCs, porous coatings could be tailored. Hence, micron-size $Fe_3O_4$NCs core mesoporous silica shell ($Fe_3O_4$@MSN) have been designed,[18, 28] $Fe_3O_4$@MSN@chitosan microspheres,[29] $Fe_3O_4$NCs@MSN foams.[30] and porous magnetite-carbon nanocapsules.[31] To our knowledge micro-sized $Fe_3O_4$@MSN materials were only tested with $Pb^{2+}$, $Cu^{2+}$, $Cd^{2+}$, $Hg^{2+}$, and $Ag^{+}$.[18, 28, 30]

In the present study, we designed $Fe_3O_4$@MSN nanocontainers functionalized with a tridentate chelate ligand for heavy metal ions removal. The functionalization was performed with a mono-alkoxysylilated derivative of diethylene triamine pentaacetic acid (DTPA). Thus excellent colloidal stability was obtained for an effective magnetic separation in aqueous media at neutral pH. The nanocontainers were found to be effective for twelve of the most toxic heavy metal ions, namely $Pb^{2+}$, $Cu^{2+}$, $Zn^{2+}$, $Cd^{2+}$, $Tl^{+}$, $Pd^{2+}$, $Ni^{2+}$, $Hg^{2+}$, $Cr^{3+}$, $Co^{2+}$, $Mn^{2+}$, and $Sn^{4+}$. Furthermore, the adsorption capacity was enhanced by taking advantage of the porosity of the mesoporous silica framework (Scheme1).

[a] *Université des Sciences et de la Technologie Houari Boumediène (USTHB), Faculté de chimie, BP: 32 El- Alia 16111 Bab Ezzouar Alger.*
[b] *Institut Charles Gerhardt Montpellier. UMR-5253 CNRS-UM2-ENSCM-UM1. cc 1701, Place Eugène Bataillon. F-34095 Montpellier cedex 05. (France). Fax: (+) 00-33-4-67-14-38-52 E-mail: jonasc@chem.ucla.edu.*
†Electronic supplementary information (ESI) available. See DOI:
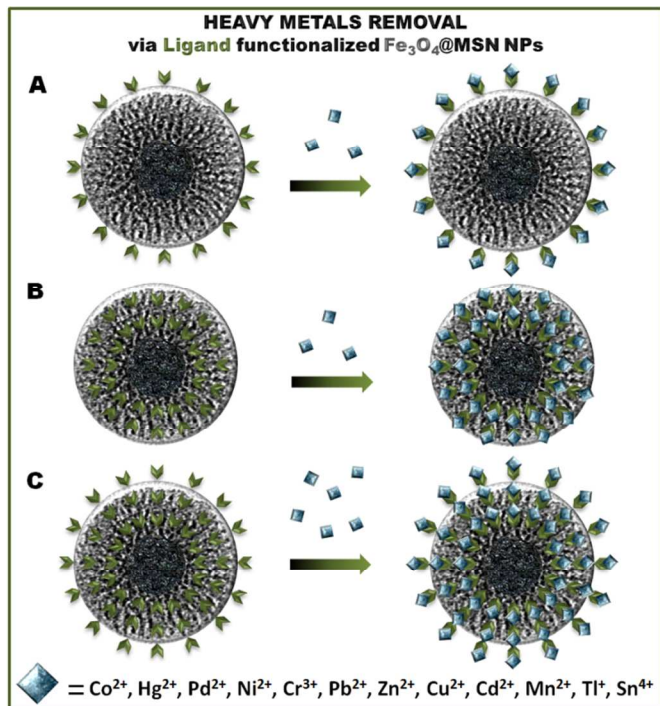
**Scheme 1** Heavy metal removal strategies: surface functionalized $Fe_3O_4$@MSN NPs (A), the porous functionalized $Fe_3O_4$@MSN NPs (B), and surface/porous functionalized $Fe_3O_4$@MSN NPs (C).

First of all, DTPA functionalized magnetic mesoporous nanocontainers were designed with different strategies (Scheme 2). Spherical $Fe_3O_4$NCs of $21\pm2$ nm were synthesized via thermal decomposition at 340°C of hydrated iron oxide with oleic acid in docosane. Then, the mesoporous silica layer was grown in a sol-gel process at 80°C with a sodium hydroxide catalyst in a cetyltrimethylammonium bromide/water mixture for 2 h. Three types of nanocontainers were obtained (Scheme 2), surface functionalized NPs ($Fe_3O_4$@MSN-L), porous functionalized NPs ($Fe_3O_4$@MSL), and the combined surface/porous functionalized NPs ($Fe_3O_4$@MSL-L). The $Fe_3O_4$@MSN-L NPs were obtained through post-functionalization of $Fe_3O_4$@MSN by the alkoxysilylated DTPA. IR spectra demonstrated the ligand functionalization (ESI Fig. S1-2), with the apparition of $\nu_{Si-C}$ at 1204 cm$^{-1}$, $\nu_{N-C}$ at 1398 cm$^{-1}$, $\nu_{C=O}$ at 1644 cm$^{-1}$, and $\nu_{C-C}$ from at 1888 to 1942 cm$^{-1}$ vibration modes corresponding to the DTPA. Solid state nuclear magnetic resonance (NMR) $^{13}$C and $^{29}$Si CPMAS spectra on a control of ligand functionalized MSN NPs further confirmed the surface functionalization (Fig. S3). Elemental analysis and energy dispersive spectroscopy quantitative composition determinations measured 37.8 and 31.0 wt% of ligand functionalization respectively (ESI Fig. S4). The porous functionalization of $Fe_3O_4$@MSL was constructed in two steps. Initially, a mixture of the tetraethoxysilane silica precursor (TEOS) and (3-aminopropyl)trimethoxysilane moiety was condensed on $Fe_3O_4$NCs, leading to iron oxide core mesoporous amino-silica shells ($Fe_3O_4$@MSNH$_2$, see scheme 2). Then, the DTPA precursor was reacted in the pores to obtain $Fe_3O_4$@MSL NPs. This grafting is also supported by the IR spectra of $Fe_3O_4$@MSNH$_2$ and $Fe_3O_4$@MSL, with the disappearance of the sharp $\nu_{N-C}$ vibration band at 1385 cm$^{-1}$, and the appearance of the $\nu_{C=O}$ at 1631 cm$^{-1}$, and the $\nu_{C-C}$ at 1850-1961 cm$^{-1}$ (ESI Fig. S5-6). Finally, $Fe_3O_4$@MSL-L was designed via the grafting of the alkoxysilylated DTPA on $Fe_3O_4$@MSL nanocontainers.
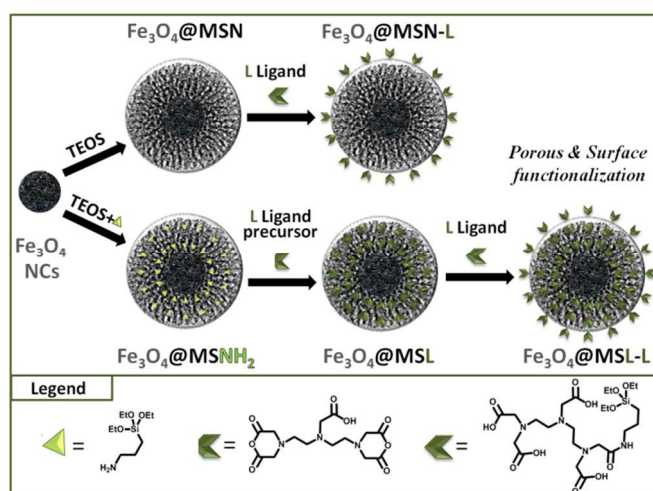


**Scheme 2** Synthetic pathways to design ligand functionalized $Fe_3O_4$@MSN NPs.

The $Fe_3O_4$@MSN nanocontainers were characterized via transmission and scanning electron microscopies (Fig. 1A-B). Spherical radial mesostructures were observed, and most nanocontainers were composed of a 20 nm iron oxide core, leading to an overall size of 130 nm. The size monodispersity of the NPs was confirmed by dynamic light scattering (DLS) measurements (Fig. 1D). The mesoporous framework was analyzed via nitrogen-adsorption-desorption technique, and the typical type IV isotherm profile was acquired (Fig. 1E). A surface area of 530 m$^2$/g was calculated by the BET theory, and a pore diameter of 3 nm was determined. Similarly, the $Fe_3O_4$@MSNH$_2$ nanocontainers were fully characterized and found to be 50 nm monodisperse and non-aggregated mesoporous NPs (ESI Fig. S7).

The heavy metal ions removal was then magnetically carried out with $Fe_3O_4$@MSN-L NPs (Fig. 2). All the experiments were performed in aqueous media at neutral pH. The nanocontainers were mixed in deionized water with various metal salts excess to continually saturate the solution, and the solution was stirred overnight at room temperature. Afterwards, a magnet was placed on the side of the reaction tube for 10 minutes, the supernatant and the metal salts were removed. Finally, the NPs were washed thrice in water, twice in ethanol, and once in acetone, to remove the non-adsorbed metal residues (see ESI Fig. S8).
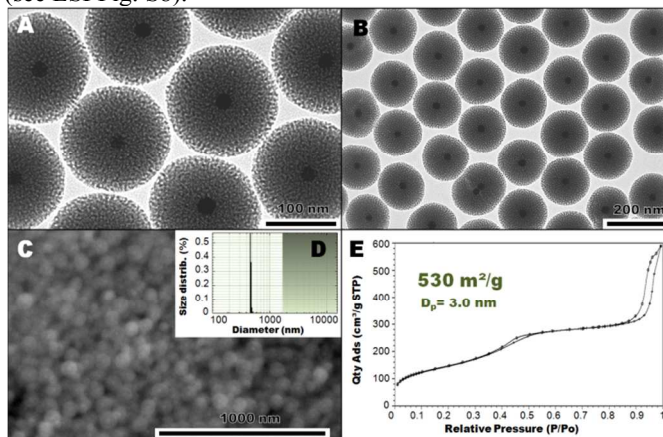


**Fig. 1** Transmission and scanning electron microscopy of $Fe_3O_4$@MSN NPs (A-B, C respectively), the DLS size distribution (D), and N$_2$-adsorption-desorption analysis (E).
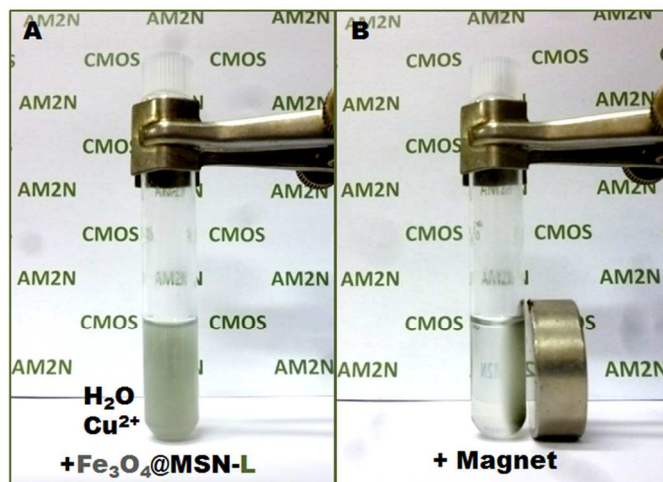
**Fig. 2** Nanocontainers, before (A) and after magnetic separation of $Fe_3O_4$@MSN-L$\cap$Cu$^{2+}$ NPs (B).



**Fig. 3** Heavy metal removal capacities of t $Fe_3O_4$@MSN-L NPs.

The metal adsorption capacities (Fig. 3) were determined by statistical energy dispersive spectroscopy measurements (ESI, Fig. S9, Table S1-12). Interestingly, the ligand functionalized nanocontainers were found to be a versatile platform for many different kinds of metals. Moreover, such a separation was very efficient for certain metal ions, such as palladium(II), copper(II), chromium(III), tin (IV), nickel(II), and zinc(II), with adsorption capacities ranging from 1000 to 2400 $\mu mol.g^{-1}$. Note that, the absence of chloride on the EDS spectra for most of NPs using metal chloride precursors validates the adsorption-washing procedure that was used to remove precipitated salts. Not surprisingly, the exceptions are the magnetic chromium chloride as well as the very soluble palladium chloride, probably partly accumulated in the pores. Thus, comparing solely the surface adsorption capacities of coated iron oxide nanocontainers (to avoid iron ions pollution), our system is very competitive with the current literature. Comparing surface functionalized amino-MSN with $Fe_3O_4$@MSN-L nanocontainers, the adsorption of Ni$^{2+}$, Cd$^{2+}$, and Pb$^{2+}$ was nearly doubled.[21] Consequently, the DTPA ligand is most appropriated to pollutant removal green materials and nanomaterials. Moreover, the selectivity of the ion removals was studied and found to be preferential towards palladium (58%), copper (21%), and lead (7%) in a mixture of all types of metals (Fig. S10) which further illustrates the applicability of these nanocontainers.

The metal ions could then be removed *via* acidic treatment, as reported in the literature.[28] At pH 4.5 the efficiency of the nanocontainers regeneration was 90 and 99% for copper and zinc ions respectively after one desorption process, according to inductively-coupled plasma analysis (Fig. S11). Note that, the iron oxide weight percent remained unchanged after the acidic extraction, thus showing the stability of the core thanks to the silica protective layer. Besides, the removal was found to be reversible with 99% efficiency after 2 cycles (Fig. S12).
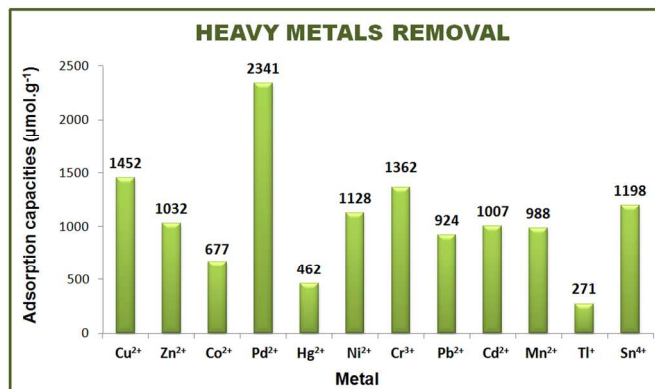
The enhancement of the adsorption capacities was considered for copper and zinc ions. The three types of ligand functionalized nanocontainers, $Fe_3O_4$@MSN-L, $Fe_3O_4$@MSL, and $Fe_3O_4$@MSL-L were compared (Fig. 4). Surprisingly, the adsorption capacities of $Fe_3O_4$@MSL were smaller than that of $Fe_3O_4$@MSN-L, with 503 and 570 $\mu mol.g^{-1}$ of zinc and copper respectively in the former, and 797 and 1122 $\mu mol.g^{-1}$ in the later. This may be due to steric pore hindrance of amine groups which lowered the porous surface, as well as the steric effect occurring when partial metal adsorption has occurred. However, the combination of the surface and porous ligand grafting in $Fe_3O_4$@MSL-L led to proportional enhancement of the adsorption capacities, reaching 1363 and 1904 $\mu mol.g^{-1}$ of zinc and copper respectively. In both cases, an additional 40 percent of metal ions was adsorbed. Note that, the correlation between the amount of ligand and the adsorbed quantity of heavy metals was confirmed by varying the amount of DTPA in the pores and on the surface (ESI Fig. S13). Furthermore, the metals ions were not merely physically entrapped in the MSN framework, as suggested by the 5 to 9 cm$^{-1}$ shifts in the carbonyl vibration modes (ESI Fig. S14-17). Besides, the observed increase of the intensity of the $\nu_{C=O}$ bands is in accord with conformational change associated with the DTPA-M$^{n+}$ complex formations. That is why various colors were observed for each type of metal complexes in the NPs framework.
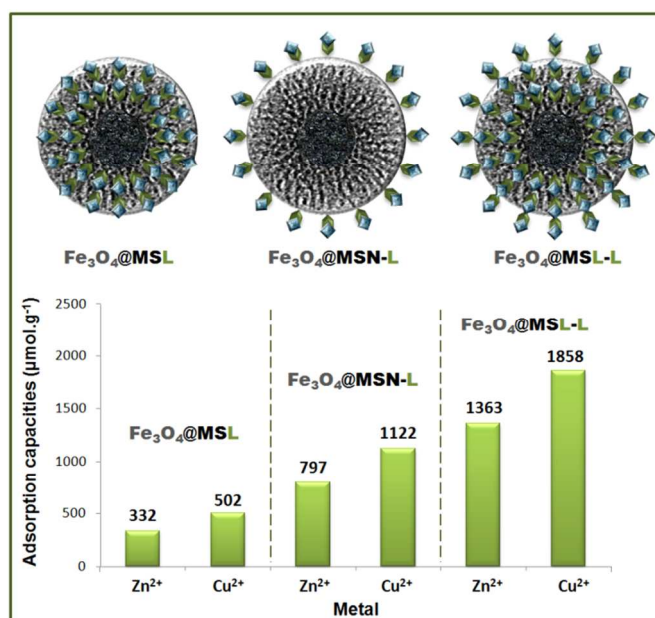
**RSC Advances Accepted Manuscript**

**Fig. 4** Heavy metal removal capacities optimization of the various nanocontainers strategies.

## Conclusions

In summary, we have developed a novel diethylene triamine pentaacetic acid ligand functionalized with monodisperse $Fe_3O_4@MSN$ and $Fe_3O_4@MSNH_2$ nanocontainers. Such NPs were found to be capable of a versatile and efficient magnetic separation on a dozen of heavy metal ions. The adsorption capacities tended to be higher for the metal having high valence and electronic affinities, such as $Pd^{2+}$ (2341 $\mu mol.g^{-1}$), $Co^{2+}$ (1452 $\mu mol.g^{-1}$), $Cr^{3+}$ (1362 $\mu mol.g^{-1}$), $Sn^{4+}$ (1198 $\mu mol.g^{-1}$), and $Ni^{2+}$ (1128 $\mu mol.g^{-1}$). Palladium(II), copper(II), and lead(II) ions were selectively removed in a mixture of all types of ions, which makes the nanocontainers selective platforms for heavy metal removal. Besides, the nanocontainers could be regenerated and reused with high efficiencies. Additionally, the adsorption capacities have been enhanced of 40 percent by the porous and surface functionalization of the nanocontainers. We are currently investigating the optimization of the adsorption capacity with larger pores and higher surface areas, in order to avoid the steric hindrance inside the mesopores. It is envisioned that such $Fe_3O_4@MSL-L$ NPs could be powerful tools to efficiently clear heavy metal liquid waste.

## Acknowledgments

**RSC Advances Accepted Manuscript**

## Notes and references

1. L. Järup, *Br. Med.l Bull.,* 2003, **68**, 167-182.
2. X. Liu, Q. Song, Y. Tang, W. Li, J. Xu, J. Wu, F. Wang and P. C. Brookes, *Sci. Tot. Environ.*, 2013, **463-464**, 530-540.
3. M. Pizzol, P. Christensen, J. Schmidt and M. Thomsen, *J. Clean. Prod.*, 2011, **19**, 646-656.
4. N. Malik, A. K. Biswas, T. A. Qureshi, K. Borana and R. Virha, *Environ. Monit. Assess.*, 2010, **160**, 267-276.
5. F. Fu and Q. Wang, *J. Environ. Manag.*, 2011, **92**, 407-418.
6. J. S. Barbosa, T. M. Cabral, D. N. Ferreira, L. F. Agnez-Lima and S. R. Batistuzzo de Medeiros, *Ecotoxicology and Environmental Safety*, 2010, **73**, 320-325.
7. T. C. O. T. E. Communities, *Off. J. Eur. Comm.*, 2000, **226**, 3.
8. S. H. Laura D. K. Thomas, Mark Nieuwenhuijsen and Lars Jarup, *Environ. Health Perspect.*, 2009, **117**, 181-184.
9. N. Johri, G. g. Jacquillet and R. Unwin, *BioMetals*, 2010, **23**, 783-792.
10. Q. Gu and R.-L. Lin, *J. Appl. Physiol.*, 2010, **108**, 891-897.
11. K. Gulati, B. Banerjee, S. B. Lall and A. Ray, *Ind. J. Exp. Biol.*, 2010, **48**, 710-721.
12. M. Y. Vilensky, B. Berkowitz and A. Warshawsky, *Environ. Sci. Technol.*, 2002, **36**, 1851-1855.
13. W. Plazinski and W. Rudzinski, *Environ. Sci. Technol.*, 2009, **43**, 7465-7471.
14. G. Mahajan and D. Sud, *J. Environ. Chem. Eng.*, 2013, **1**, 1020-1027.
15. M. A. Hasan, Y. T. Selim and K. M. Mohamed, *J. Haz. Mater.*, 2009, **168**, 1537-1541.
16. B. Yu, Y. Zhang, A. Shukla, S. S. Shukla and K. L. Dorris, *J. Haz. Mater.*, 2000, **80**, 33-42.
17. W. S. Wan Ngah, L. C. Teong, R. H. Toh and M. A. K. M. Hanafiah, *Chem. Eng. J.*, 2013, **223**, 231-238.
18. G. Li, Z. Zhao, J. Liu and G. Jiang, *J. Haz. Mater.*, 2011, **192**, 277-283.
19. M. Hua, S. Zhang, B. Pan, W. Zhang, L. Lv and Q. Zhang, *J. Haz. Mater.*, 2012, **211-212**, 317-331.
20. J. Wang, Y. Shao, J. Liu, Z. Xu and D. Zhu, *J. Col. Interface Sci.*, 2010, **349**, 293-299.
21. M. Najafi, Y. Yousefi and A. A. Rafati, *Sep. Purif. Technol.*, 2012, **85**, 193-205.
22. M. Chen, Y. Liu and Y. Hao, *Chem. Eng. J.*, 2013, **218**, 48-54.
23. S. Dib and M. Boufatit, *Desalination*, 2009, **5**, 106-110.
24. F. Mohammed-Azizi, S. Dib, and M. Boufatit, *Desalination*, 2013, **51**, 4447-4458.
25. H. Assameur and M. Boufatit, *Desalination, ,*2012, **45**, 315-323.
26. L. Wang, J. Li, Q. Jiang and L. Zhao, *Dalton Trans.*, 2012, **41**, 4544-4551.
27. P. Xu, G. M. Zeng, D. L. Huang, C. L. Feng, S. Hu, M. H. Zhao, C. Lai, Z. Wei, C. Huang, G. X. Xie and Z. F. Liu, *Sci. Tot. Environ.*, 2012, **424**, 1-10.
28. Q. Yuan, N. Li, Y. Chi, W. Geng, W. Yan, Y. Zhao, X. Li and B. Dong, *J. Haz. Mater.*, 2013, **254-255**, 157-165.
29. Y. Ren, H. A. Abbood, F. He, H. Peng and K. Huang, *Chem. Eng. J.*, 2013, **226**, 300-311.
30. J. Chung, J. Chun, J. Lee, S. H. Lee, Y. J. Lee and S. W. Hong, *J. Haz. Mater.*, 2012, **239-240**, 183-191.
31. K. Cheng, Y.-M. Zhou, Z.-Y. Sun, H.-B. Hu, H. Zhong, X.-K. Kong and Q.-W. Chen, *Dalton Trans.*, 2012, **41**, 5854-5861.

$Co^{2+}$ $Hg^{2+}$ $Pd^{2+}$ $Ni^{2+}$ $Cr^{3+}$ $Pb^{2+}$
$Zn^{2+}$ $Cu^{2+}$ $Cd^{2+}$ $Mn^{2+}$ $Tl^{+}$ $Sn^{4+}$

200 nm

$Fe_3O_4$@MSN-DTPA NPs